

Improve Thermal Behavior of Thin Polyimide Films Using Infrared Spectroscopy Analysis and Electrical

Fathi Etaher Elbakoush, Kamal Farag Alhauwari, Mohamed Shaban

College of science and Technology, Surman, Libya, Faculty of Natural Resources Engineering, University of Zawia
Fathi808@scst.edu.ly, k.alhauwari@zu.edu.ly, Moh_tub@scst.edu.ly

Abstract— It is investigated how increasing temperature affects the molecular structure as well as the thermal and electrical properties of polyimide thin films. FTIR spectroscopy and changes in the extent of imidization are used to investigate the effects of increasing temperature on the formation of imide rings. However, this technique has a poor accuracy in determining the optimal imidization temperature. As a result, quantifying several electrical properties used as probes of the imidization reaction advancement (particularly high field electrical measurements) allows for the greatest accuracy in determining the optimal imidization temperature. An optimum temperature is found at 400 °C while desimidization is observed at 450 °C. This is in agreement.

Keywords— Temperature, film, quantifying several electrical, . FTIR spectroscopy.

I. INTRODUCTION

With the increased use of polymers in the microelectronic industry, a microscopic understanding of the mechanism underlying metal-polymer adhesion has grown in importance. Polyimide (PI) is well known and extensively studied in the field of high performance engineering plastic materials due to its excellent thermal and mechanical properties, making it one of the polymers suitable for microelectronic applications. Aircraft parts, aerospace applications, electronic packaging, adhesives, and matrix materials for composites are among the industrial applications for PI-based materials [1]. Polyamides have been widely used in microelectronics as dielectric spacing layers, protective coatings, and substrates for metal thin films for all of these reasons, replacing traditional inorganic insulators such as SiO₂ in many applications. Good adhesion between polyimide and a metal substrate, as well as between individual metal atoms and a polyimide substrate, is required in these and other applications. Though chemical bonding at the interface is thought to be important in adhesion, the mechanism underlying adhesion is frequently unknown. The way the interface is formed has a direct impact on interfacial bonding and, consequently, adhesion. Variations in polymer or metal substrate preparation can thus result in polyimide/metal interfaces with varying adhesive strength. The study of metal-polymer adhesion has the potential to advance significantly with a better comprehension of the chemical interactions at metal/polyimide interfaces and their effects on adherence. Similar to other disciplines, atomistic modeling can be helpful in comprehending how metal-polyimide bonds arise. Because chemical interaction at interface formation causes flexible polymer distortion, a simultaneous self-consistent

calculation of both electronic structure and molecular geometry of the entire absorbate-substrate system is required.

High temperature electronics and power electronics applications have emerged in recent years, necessitating the use of wide band gap semiconductors (SiC, GaN, and diamond). Such devices subject packaging materials to higher operating temperatures (N200 °C), such as polyimide (PI) surface passivation [2]. The classical PMDA/ODA PI appears insufficient for enduring thermal constraints due to the degradation of the C-O-C ether bond present in the monomer unit [3, 4] in this high temperature range of operation. Consequently, PIs derived from biphenyltetracarboxylic dianhydride (BPDA) and p-phenylene diamine (PDA), which have greater thermal stability than PMDA/ODA [3, 4], appear to be a promising candidate. However, little is known about the imidization of BPDA/PDA [5]. The final physical properties of PIs, as well as their integrity over time, are heavily dependent on the control and optimization of the imidization reaction (i.e. the curing process) [6, 7]. This procedure appears to be critical for industrial applications. Unfortunately, predicting the optimal imidization temperature that results in the best electrical properties is difficult. Between 200 and 425 °C of imidization temperatures are presented in the literature, however it is not always clear whether or not each temperature corresponds to an optimum [7–13]. This paper discusses the effect of imidization temperature on the molecular structure, thermal, and electrical properties of BPDA/PDA thin films. A specific accurate methodology based on the analysis of the electrical properties under various electrical setups and as a function of the imidization temperature is reported in order to optimize this process step.

II. EXPERIMENTAL

II.1. Materials.

The BPDA/PDA PI was purchased in the form of a poly (amic acid) (PAA) solution. It was synthesized in two steps using precursor monomers such as BPDA dianhydride and PDA diamine [14]. The PAA solution was made by dissolving the precursor monomers in N-methyl-2-pyrrolidone, an organic polar solvent (NMP). At 25 °C, the PAA solution had a viscosity of 27 poises and a density of 1.064 g cm³. To convert PAA to PI, the solution was heated to remove NMP and induce imidization via water molecule evaporation. (Fig1) depicts the BPDA/PDA synthesis steps.

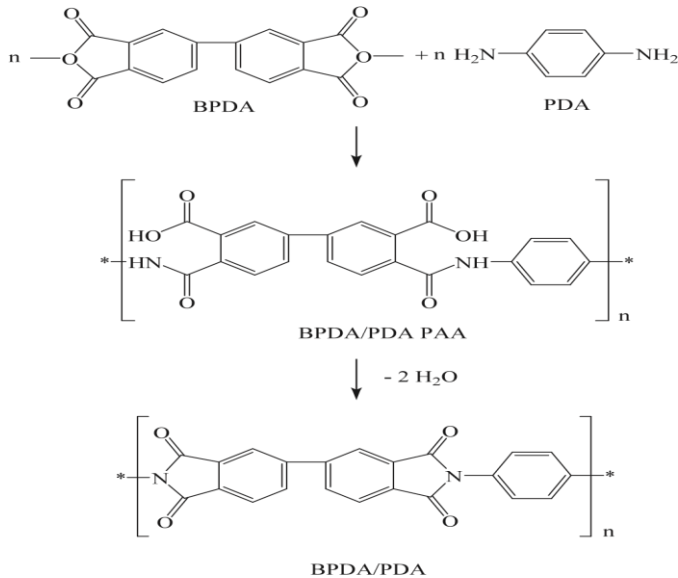


Fig. 1: Synthesis steps of the BPDA/PDA polyimide.

II.2. Film and sample preparation.

On square stainless steel substrates, the PAA solution was spin-coated (16 cm²). It was spread at 500 rpm for 10 seconds, and then spun at 4000 rpm for 30 seconds. The coatings were followed by two curing steps. Following a soft-bake (SB) at a low Differential scanning calorimetry (DSC) measurements were performed using a Netzsch 204 calorimeter at a heating rate of 10 °C min⁻¹ up to 500 °C under helium. A Bio-Rad FTS-60A infrared spectrometer in attenuated total reflection mode was used for the Fourier transform infrared (FTIR) analysis. A reflection cell with a 60° incidence angle was used. Each sample received an average of 128 scans ranging from 400 to 4000 cm⁻¹. 4 cm⁻¹ was the resolution. The uncoated substrates were measured as the "background" spectra prior to any measurements and were automatically subtracted from each scan. Because all spectra were normalized to the typical 1500 cm⁻¹ C=C absorption band, the following scans were baseline-corrected. Three techniques were used for electrical characterizations: dielectric relaxation spectroscopy (DRS), conduction current (CC), and breakdown strength (BS) experiments. DRS was performed from 101 to 106 Hz using a Novo control Alpha-A spectrometer, measuring the dielectric loss factor (tan) and alternative conductivity (AC) as a function of imidization temperature. A Keithley electrometer (6517A with an integrated static voltage source) and a Keithley source meter (SM 2410 with an integrated sweep voltage source) were used for the CC and BS measurements, respectively. At room temperature, all electrical measurements were taken. Coatings were hard-cured (HC) at a higher temperature (THC) under a nitrogen atmosphere and for a time THC at a temperature (TSB) of 150 °C for 3 minutes on a hot-plate in air. The THC temperature is thus defined as the imidization temperature in the following sections. According to the THC, the final film thicknesses were measured using a KLA Tencor Alpha-Step IQ profilometer in the range of 1.3 to 2.2 μm. Under vacuum (104 Pa), an upper gold metallization was evaporated onto the PI film surface to perform the electrical measurements. This metal layer was then patterned using a photolithography step (via a

selective mask) followed by a humid gold etching to form circular electrodes ranging in diameter from 1 to 5 mm.

II.3. Details of the curing parameters.

The imidization cure is required to drive off the solvent (boiling point of 200 °C for NMP) and convert PAA to PI via imide ring formation. PAA coatings were hard-cured at THC ranging from 175 to 450 °C under nitrogen in an SPX Blue M IGF 6680 programmable oven for 60 minutes. All of the samples had heating and cooling rates of 2.5 and 4 °C min⁻¹, respectively.

II.4. Measurements.

A Perkin Elmer Instrument analyzer with 10 g accuracy was used for dynamic thermogravimetric analysis (DTGA). Weight losses were measured on both PAA and PI films (10 mg) stripped from their substrates. Temperatures up to 1000 °C were measured in both air and nitrogen atmospheres, with a heating rate of 10 °C min⁻¹.

III. RESULTS AND DISCUSSION

III.1. Thermal properties of BPDA/PDA PAA and PI films.

DSC and DTGA were used to investigate the thermal properties of PAA coatings during cyclization into PI films. The DSC thermogram of PAA coatings at temperatures ranging from 25 to 400 °C after SB at 150 °C is shown in Fig. 2(a). The precursor polymer has a large endothermic peak at 196 °C and a high enthalpy value of 139 J g⁻¹.

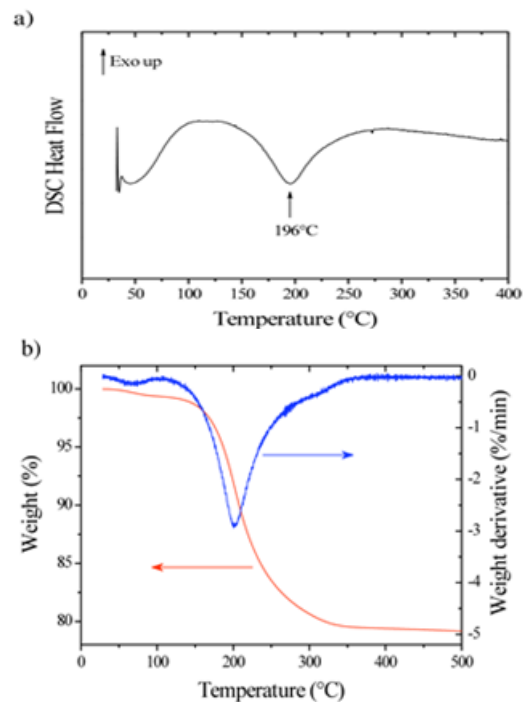


Fig. 2. DSC (a) and DTGA (b) thermograms of the BPDA/PDA PAA coating after the SB at 150 °C. Heating rate: 10 °C/min; atmospheres: (a) in He and (b) in N₂.

This peak is primarily caused by the removal of the NMP solvent from the coating at around 200 °C during vaporization. However, this peak is also likely due to water molecule

evaporation when the imidization reaction begins [6, 15, and 16]. The evaporation of both the solvent and the H₂O is usually associated with a significant decrease in the weight of the initial coating (several). The DTGA thermogram of PAA coatings during conversion into PI is shown in Fig. 2(b). When the temperature is raised to 350 °C, the weight changes by about 20%. The maximum weight loss speed is located near 200 °C and is related to the NMP boiling point. The slight changes in weight losses above 350 °C may indicate complete evaporation of the water and solvent. The thermal stability of PI films was determined using DTGA, as indicated by weight losses at high temperatures.

Fig. 3 depicts typical DTGA thermograms of BPDA/PDA PI films in both nitrogen and air atmospheres for THC_s greater than 300 °C. A comparison with conventional PMDA/ODA thin films is also provided. In nitrogen and air atmospheres, the thermal stability of BPDA/PDA is defined as 606 °C and 584 °C, respectively. For nitrogen and air atmospheres, the thermal stability of PMDA/ODA appears to be 60 °C and 110 °C lower than that of BPDA/PDA. The earlier occurrence of weight loss in air is related to thermo-oxidation degradation of the macromolecular structure [2,17]. Furthermore, the chemical structure of PIs' monomer unit is closely related. To their thermal stability. The higher thermal stability of BPDA/PDA can be attributed primarily to the higher thermal stability of the PDA diamine in comparison to the ODA

diamine found in PMDA/ODA. The absence of the C-O-C ether function in BPDA/PDA causes it to degrade more quickly than PMDA/ODA [2, 4].

III.2. Fourier transform infrared (FTIR) analysis of PAA and PI films.

To detect chemical bond changes during the imidization of PAA into PI, absorption band assignments in FTIR spectra are required to identify the amide and imide peaks.

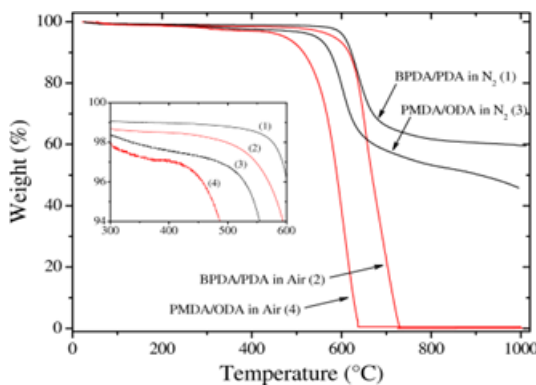


Fig. 3. Typical DTGA thermograms of the BPDA/PDA and PMDA/ODA in N₂ and air Atmospheres after a THC_s ≥ 300 °C. Heating rate: 10 °C min⁻¹.

Previous work [5, 6, 16, 18-27] was used to assign the characteristic IR absorption peaks. The common absorption vibrational modes and their most likely origin for PAA, PI, and NMP solvents are listed in Table 1. The N-H stretch bonds at 2900-3200 cm⁻¹, the C=O carbonyl stretch from carboxylic acid at 1710-1720 cm⁻¹, the symmetric carboxylate stretch bonds at 1330-1415 cm⁻¹, the C=O carbonyl stretch of the amide I mode around 1665 cm⁻¹, the 1540-1565 cm⁻¹ amide II mode, and the

1240-1270 cm⁻¹ band due to the C-O-C ether aromatic stretch are typical PAA spectra (if present in the monomer). The absence of absorption bands near 1550 cm⁻¹ (amide II) and 1665 cm⁻¹ (amide I) after the conversion reaction indicates that PAA has been converted into PI. This is confirmed by the simultaneous occurrence of the C=O stretch (imide I) peaks at 1770-1780 cm⁻¹ (symmetric) and 1720-1740 cm⁻¹ (asymmetric), the typical C-N stretch (imide II) peak around 1380 cm⁻¹, the C-H bend (imide III) and C=O bend (imide IV) absorption bands in the ranges of 1070-1140 cm⁻¹ and 720-740 cm⁻¹. The C-H stretch bonds are responsible for the presence of a large absorption band in PI films between 2900 and 3100 cm⁻¹.

TABLE 1: Typical bond assignments in PI and PAA FTIR spectra.

Group	Absorption frequency(cm ⁻¹)	Vibration mode	Vibration mode
polyimide	imide I	2900-3100	C=H stretch
		1770-1780	C=O sym. stretch
		1720-1740	C=O sym. stretch
	Aromatic cycle	1500-1520	C=C stretch
	Imide II	1360-1380	C-N stretch
	Imide III	1070-1090 (and/or 1120-1140)	C-H bending
PAA	Imide IV	720-740	C=O bending
	Ether bond	120-1270	C-O-C stretch
		2900-3200	COOH and NH ₂
	Carbonyl from carboxylic acid	1710-1720	C=O(COOH) stretch
	Amide I	1660-1665	C=O(CONH) stretch
	Carboxylate ion	1600-1665	COO ⁻ asym. stretch
	Amide II	1540-1565	C-NH
	Carboxylate ion	1330-1415	COO sym. stretch
	Ether bond	1240-1270	C-O-C stretch
	Amide IV	830-890	O=C-O or O=C=N

Finally, the measurements may highlight the presence of a shoulder on the asymmetric C=O stretch bonds at 1710 cm⁻¹, which corresponds to the imide I conformation's out-of-plane optical response [28]. The FTIR spectra of PAA coatings after SB at 150 °C and PI films after HC at 250 °C are shown in Fig. 4. The spectra have been normalized to 1518 cm⁻¹ for the classical C=C absorption band. The spectrum obtained following the SB demonstrates the typical absorption bands of PAA coatings. The large absorption band seen between 2300 and 3400 cm⁻¹ corresponds to the N-H stretch vibration modes, C-H stretch bonds, and O-H stretch bonds found in both the PAA and NMP solvents. The presence of the four absorption bands from the imide rings in the FTIR spectrum of PI films indicates the typical completion of the imidization reaction. They are found at 1775/1734 cm⁻¹ (imide I), 1371 cm⁻¹ (imide II), 1124/1080 cm⁻¹ (imide III), and 737 cm⁻¹ (imide IV) (imide IV). Furthermore, the large absorption band induced by the C-H stretch vibration modes can be seen between 2600 and 3100 cm⁻¹. At 1415cm⁻¹, Near the C-N stretch peak, a shoulder appears. The symmetric stretch of the carboxylate ion COO could be responsible for this absorption band. The carboxylic

acid groups in PAA are visible at 3400 cm⁻¹ via the O-H stretching bonds, but free carboxylic acid groups can be deprotonated by the weak amine base [19]. As a result, COO carboxylate ions are commonly found in PIs, with two peaks at 1606 and 1415 cm⁻¹. This could account for the release of mobile H⁺ protons (from COOH), which is responsible for electrical conduction in PI [29].

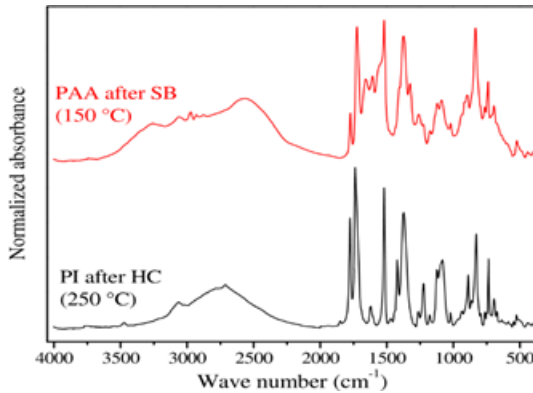


Fig. 4. FTIR spectra of both the BPDA/PDA PAA coatings and BPDA/PDA PI films.

III.3. Influence of the imidization temperature on the molecular structure of BPDA/PDA.

To determine the progress of the imidization reaction of the PI films, FTIR measurements were performed for various imidization temperatures THC. This analysis is based on changes in the magnitude of the absorption peak in the functional groups or characteristic linkages during the reaction. The changes in the FTIR spectra of BPDA/PDA for different imidization temperatures are shown in Fig. 5. When THC levels rise, all of the absorption peaks rise in unison. This implies that residual PAA monomers are still being converted into PI. After being exposed to temperatures above 350 °C, this evolution becomes stable. Investigating the imidization kinetics of PI films, the aromatic ring (C=C) peak stretching around 1500 cm⁻¹ is used as a reference, and the peak height method is used to calculate the amount of imide groups formed.

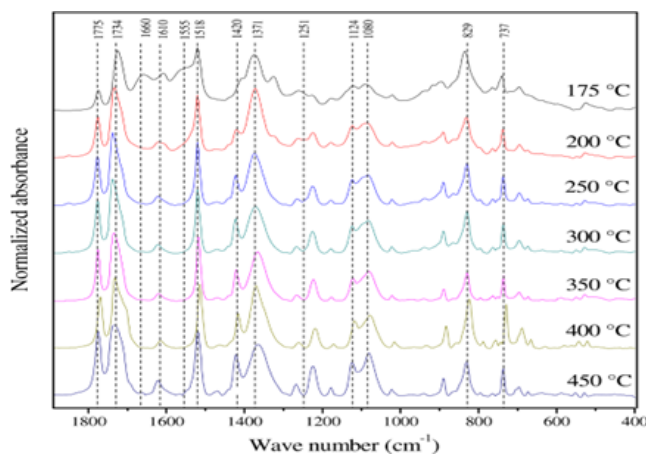


Fig. 5. FTIR spectra of the BPDA/PDA for different THC between 175 and 450 °C.

The degree of imidization (DOI) is thus defined as a comparison of the intensity of an imide absorption peak

normalized to the intensity of the C=C reference band, as shown in [16]:

$$DOI_{THC} = \frac{(A/A^*)_{THC}}{(A/A^*)_i} \quad (1)$$

Where A* is the C=C reference band peak height (1518 cm⁻¹) and A is the imide peak height (1775, 1732, 1420, 1371, 1080, and 737 cm⁻¹ in this study). The initial and given imidization temperatures are indicated by the subscripts i and THC, respectively.

Figure 6 depicts the extent of imidization of the BPDA/PDA main bonds versus the imidization temperature. The majority of the imidization reaction occurs quickly, with a conversion rate as high as 70-85% at 250 °C, and continues slightly up to 400 °C, as evidenced by an increase in the magnitude of the imide bands (cf. Fig. 6). However, difficult to determine the optimal imidization temperature (i.e. the highest magnitude) to avoid exceeding in order to protect PI from degradation. The imide II and IV absorption bands, for example, decrease by 20% and 10%, respectively, at 450 °C, indicating that the structure is being desimidized. As a result, using complementary electrical measurements as a probe of imidization advancement can provide the most accurate temperature determination.

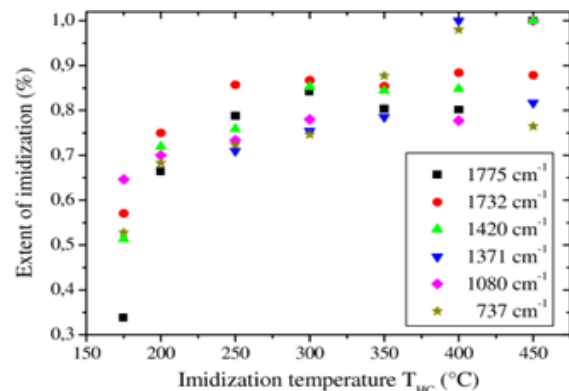


Fig. 6. Extent of the imidization reaction for the main absorption bands of the BPDA/PDA versus the imidization temperature.

III.4. Influence of the imidization temperature on the electrical properties of BPDA/PDA.

III.4.1. Study at low electric fields.

The electrical properties of the DOI are strongly influenced by the imidization temperature. Electrical conductivity, dielectric losses, and dielectric breakdown field changes in PI films can be used to precisely determine the optimal imidization temperature. Because the PI films contain less impurity, the higher the DOI, the better the electrical properties are expected. The frequency dependence of the dielectric loss factor tan (a) and the AC conductivity AC (b) of BPDA/PDA PI films for various imidization temperatures is shown in Fig. 7. THC up to 400 °C improves electrical properties significantly. In Fig. 7(a), the loss factor for a THC of 200 °C (higher than 102 in the entire frequency range) decreases to values close to 10⁻³ for THC of 350 and 400 °C.

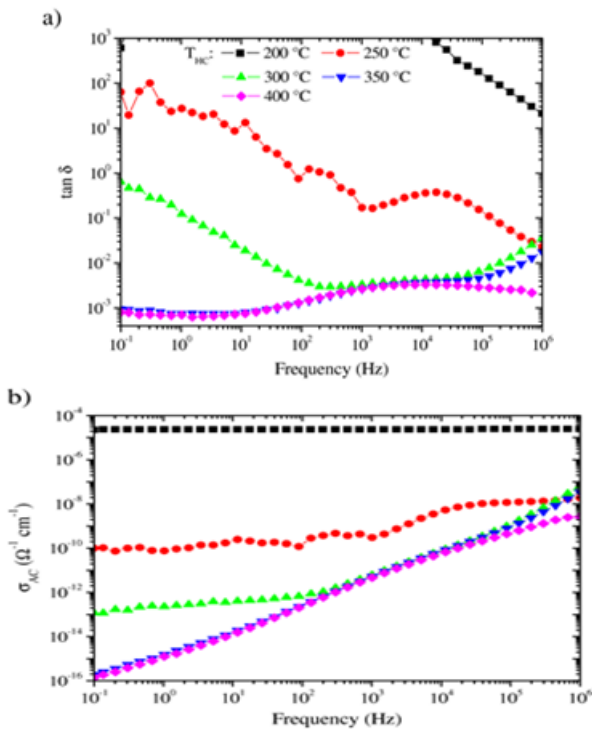


Fig. 7. Frequency dependences of the dielectric loss factor $\tan \delta$ (a) and the AC conductivity σ_{AC} (b) of the BPDA/PDA for different imidization temperatures (measured at 25 °C).

BPDA/PDA PI films exhibit only one dielectric relaxation phenomenon of very low magnitude in the range 102 to 106 Hz at such high imidization temperatures, whereas When the frequency dependence of the AC conductivity AC is plotted (see Fig. 7(b)), the conduction phenomenon occurs through a "plateau" of AC, indicating that the dielectric losses are dominated primarily by charge transport in the PI bulk. The magnitude of the "plateau" is proportional to the magnitude of static conductivity DC ($\sigma_{AC} = \sigma_{DC} + A$, where A is a constant parameter and is the pulsation) [30]. The changes in the DC (data extracted from Fig. 7(b) at 101 Hz) as a function of the imidization temperature THC are shown in Fig. 8. BPDA/PDA PI films exhibit only one dielectric relaxation phenomenon of very low magnitude in the range 102 to 106 Hz at such high imidization temperatures, whereas When the frequency dependence of the AC conductivity AC is plotted (cf. Fig. 7(b)), the conduction phenomenon occurs through a "plateau" of AC, indicating that the dielectric losses are primarily dominated by the AC conductivity. When THC is increased from 200 to 400 °C, DC is significantly increased (from 10^{-5} to $10^{-16} \Omega^{-1} \text{cm}^{-1}$). Given the low values of the applied electric field (2 kV/cm rms), there is no significant difference for THC 350 °C; however, the plateau value is not reached, and the DC values should be lower.

III.4.2. Study at high electric fields.

To clearly show the differences in the electrical characteristics of BPDA/PDA PI films formed for the THC over 350 °C, higher electric field characterizations are needed. CC measurements were made up to 1 MV/cm, and σ_{DC} values at high fields were calculated using the current density/electric field characteristics $j = \sigma_{DC} E$ (cf. Fig. 9).

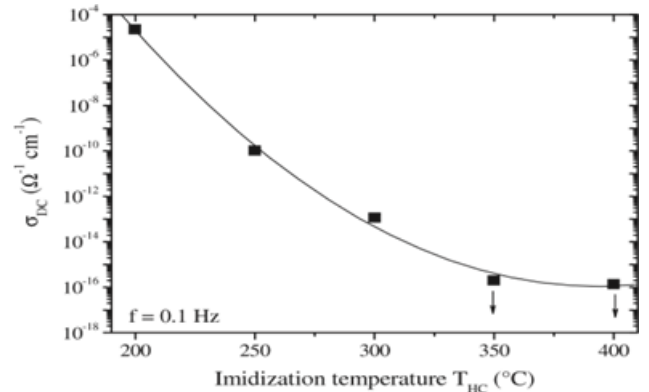


Fig. 8. Changes in the DC conductivity σ_{DC} of the BPDA/PDA versus the imidization temperature (measured at 25 °C).

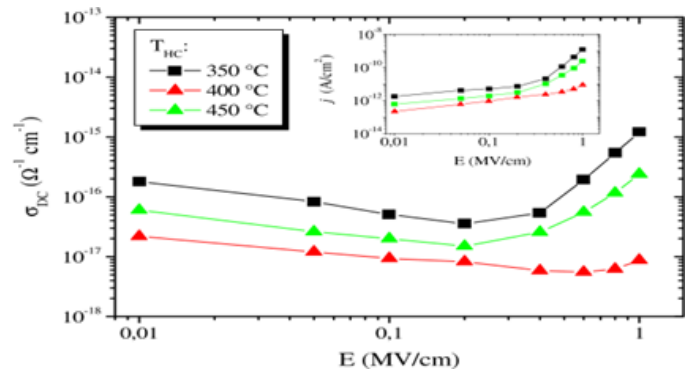


Fig. 9. Evolution of the DC conductivity of the BPDA/PDA versus the applied electric field for THC between 350 and 450 °C. The inset plot gives the electric field dependence of the conduction current density (measured at 25 °C).

Whereas σ_{DC} values are poorly distributed (with very low values) between 10^{-17} and $10^{-16} \Omega^{-1} \text{cm}^{-1}$ up to 200 kV/cm. Whatever THC was used, there was a significant divergence at high fields, where the highest insulation quality (i.e. the lowest σ_{DC}) was obtained for the films imidized at 400 °C. Thus, with this optimal imidization temperature, the density of the charges (or their mobility) appears to be significantly reduced. Electrical conduction in PI films is typically associated with H⁺ proton motions [29]. This is consistent with the development of the COO band's intensity, which decreases around 400 °C before rising once more at 450 °C. This point is highlighted by variations in the dielectric breakdown field EBR as a function of, after a continuous increase in EBR up to a THC of 400 °C, a sudden decrease in its magnitude when THC is raised to 450 °C. The degradation of the electrical properties above a THC of 400 °C appears as a consequence of desimidization (i.e. the decrease of the imide bands) of the BPDA/PDA structure leading to the release of free mobile charges in the bulk. For the THC below, a conduction phenomenon appears via a 1/f dependence [30]. Because of an incomplete conversion of PAA into PI, this occurrence is related to easier charge transports in the film.

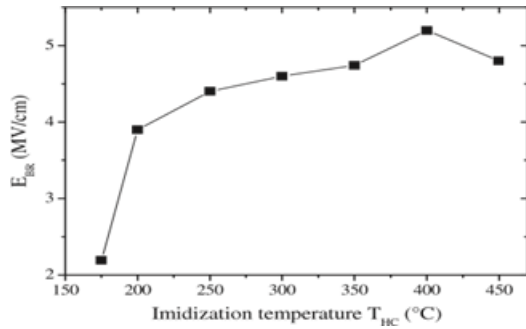


Fig. 10. Changes in the dielectric breakdown field of the BPDA/PDA versus the Imidization temperature. Each EBR value is a mean of 20 tested capacitor samples (Measured at 25 °C).

IV. CONCLUSION

The effect of imidization temperature (THC) on the molecular structure, thermal and electrical properties of BPDA/PDA polyimide films has been studied. Electrical and dielectric properties, in particular, are used as powerful probes to optimize the PI imidization reaction. The effects of imidization temperature were determined by comparing the degree of imidization extracted from FTIR spectra with the evolution of electrical and dielectric properties (electrical conductivity, dielectric loss factor and dielectric breakdown field). Whereas FTIR (350 °C) detection of the optimal imidization temperature is difficult, high field electrical measurements show an accurate determination of the optimal THC at 400 °C. As a result, using complementary electrical measurements as a probe of imidization advancement allows for the greatest accuracy in determining the optimal THC. Based on the structure-properties analysis, this methodology shows a good optimization of the imidization process step.

REFERENCE

- [1] Fathi Etaher Elbakoush; Yang Dan ; Qi Shengli ; Zhang Mengying ; Tian Guofeng ; Wang Xiaodong ; Wu Dezhen.. "Carbonization behavior of polyimide films hybrid with different metal catalyst. Polymer Science series A Journal.
- [2] S. Zemat, M.L. Locatelli, T. Lebey, S. Diahm, *Microelectron. Eng.* 83 (2006) 51.
- [3] M. Tsukiji, W. Bitoh, J. Enomoto, *Proc. Inter. Symp. Elec. Insul.* (1990) 88.
- [4] S.H. Hsaio, Y.J. Chen, *Eur. Polym. J.* 38 (2002) 815.
- [5] K.M. Chen, T.H. Wang, J.S. King, A. Hung, *J. Appl. Polym. Sci.* 48 (1993) 291.
- [6] K.P. Pramoda, S. Liu, T.S. Chung, *Macromol. Mater. Eng.* 287 (2002) 931.
- [7] T.J. Shin, M. Ree, *J. Phys. Chem. B* 111 (2007) 13894.
- [8] M. Ree, C.W. Chu, M.J. Goldberg, *J. Appl. Phys.* 75 (1994) 1410.
- [9] M. Ree, K. Kim, S.H. Woo, H. Chang, *J. Appl. Phys.* 81 (1997) 698.
- [10] S.A. Lee, T. Yamashita, K. Horie, T. Kozawa, *J. Phys. Chem. B* 101 (1997) 4520.
- [11] J. Sung, D. Kim, C.N. Whang, M. Oh-e, H. Yokoyama, *J. Phys. Chem. B* 108 (2004) 10991.
- [12] [B.J. Factor, T.P. Russell, M.F. Toney, *Phys. Rev. Lett.* 66 (1991) 1181.
- [13] T. Sasaki, H. Moriuchi, S. Yano, R. Yokota, *Polymer* 46 (2005) 6968.
- [14] C.E. Sroog, *Prog. Polym. Sci.* 16 (1991) 561.
- [15] J.H. Chang, K.M. Park, *Eur. Polym. J.* 36 (2000) 2185.
- [16] T.C.J. Hsu, Z.L. Liu, *J. Appl. Polym. Sci.* 46 (1992) 1821.
- [17] I.S. Chung, C.E. Park, M. Ree, S.Y. Kim, *Chem. Mater.* 13 (2001) 2801.
- [18] E.D. Feit, C.W. Wilkins, *Polymer Materials for Electronic Applications*, ACS
- [19] *Symposium Series 184*, American Chemical Society, Washington DC, 1982.
- [20] M. Anthamatten, S.A. Letts, K. Day, R.C. Cook, A.P. Gies, T.P. Hamilton, W.K. Nonidez, *J. Polym. Sci. A Polym. Chem.* 42 (2004) 5999.
- [21] H. Ishida, S.T. Wellinghoff, E. Baer, J.L. Koenig, *Macromolecules* 13 (1980) 826.
- [22] B. Thomson, Y. Park, P.C. Painter, R.W. Snyder, *Macromolecules* 22 (1989) 4159.
- [23] R.W. Synder, B. Thompson, B. Bartges, D. Czerniawski, P.C. Painter, *Macromolecules* 22 (1989) 4166.
- [24] C.A. Pryde, *J. Polym. Sci. A Polym. Chem.* 31 (1993) 1045.
- [25] I. Karamancheva, V. Stefov, B. Soptrajanov, G. Danev, E. Spasova, J. Assa, Vib.